arXiv:cond-mat/0612559v2 [cond-mat.mtrl-sci] 26 Mar 2007

Quantum spin configurations in $Tb_2Ti_2O_7$

S. H. Curnoe*
Department of Physics and Physical Oceanography, Memorial University of Newfoundland, St. John's, Newfoundland & Labrador A1B 3X7, Canada

Low energy collective angular momentum states of the Tb^{3+} ions in $Tb_2Ti_2O_7$ are classified according to the irreducible representations of the octahedral point group. Degeneracy lifting due to the exchange interaction is discussed. Diffuse neutron scattering intensity patterns are calculated for each collective angular momentum state and the ground state is inferred by comparing to experiment.

PACS numbers:

$Tb_2Ti_2O_7$ is geometrically frustrated due to its pyrochlore crystal structure, apparently leading to a "spin liquid" state which persists to extremely low temperatures.[1] The spin liquid is characterised by an abundance of low-lying excited states which tend to prevent the formation of an ordered state because of fluctuations. The focus of experimental work has been to determine the conditions under which the spin liquid state becomes unstable against the development of long range order. Theoretical studies of antiferromagnetic interactions predict that ordering should occur with a Néel temperature of approximately 1.2 K,[2,3,4] but this is not seen experimentally. There are reports of short-range ordering occurring at $T_c = 0.37$ K[5,6] and a spin glass phase below 200 mK,[6,7,8] however one group has found that the spin liquid phase persists down to at least 50 mK.[1,9] Even in the absence of long range order, one may expect that local correlated spin configurations, possibly governed by the exchange interaction, will be present. Indeed, a diffuse neutron scattering experiment that found an intensity pattern characterised by a broad peak at $\mathbf{q} = [0, 0, 2]$[10] has been interpreted in this way.[11]

There is a vast literature of theoretical works on the general topic of spin liquids in geometrically frustrated systems.[12] A small subset of these treat the magnetic ions as classical Ising spins which point toward the corners of the tetrahedra, and this approach has been useful for understanding spin ice behaviour in the related compounds $Ho_2Ti_2O_7$ and $Dy_2Ti_2O_7$.[3,13] In this article, we extend this approach using basic considerations of symmetry and quantum mechanics.

$Tb_2Ti_2O_7$ crystallises in the pyrochlore structure with space group $Fd\bar{3}m$ (#227, O_h^7). With two copies of the chemical formula per unit cell, there are four Tb ions which occupy the corners of a corner-shared tetrahedral network. The local site symmetry is $\bar{3}$m (D_{3d}), where the three-fold axes point along the directions [111], $[-1-11]$, $[-11-1]$ and $[1-1-1]$ for sites #1, 2, 3 and 4, respectively. In this environment, the $J = 6$ manifold of the $4f^8$ state of Tb^{3+} splits into levels labeled by the irreducible representations (IR's) of D_3: $3A_1 \oplus 2A_2 \oplus 4E$.[14] Neutron scattering measurements and *ab initio* calculations find that the ground state and first excited states are E doublets, separated by 1.5 meV.[2]

Both the ground state and first excited state are linear combinations of the angular momentum states $|\pm 5\rangle$, $|\pm 2\rangle$, $|\mp 1\rangle$ and $|\mp 4\rangle$, where the quantum numbers measure $\vec{J}$ in the direction of the C_3 axis. The ground state doublet was determined to be[2,15]

$$|\pm\rangle = \pm 0.13|\pm 5\rangle \mp 0.13|\mp 1\rangle - .97|\mp 4\rangle. \qquad (1)$$

With four Tb ions per unit cell, there is therefore a sixteen-fold degeneracy of the ground state for each unit cell. The collective angular momentum states are denoted $|\pm\pm\pm\pm\rangle \equiv |\pm\rangle_1 \otimes |\pm\rangle_2 \otimes |\pm\rangle_3 \otimes |\pm\rangle_4$, where the subscripts indicate the site number. These states are divided according to the representations by which they transform under the operations of the octahedral point group O_h, the underlying point group symmetry of the crystal, as $A_{1g} \oplus 3E_g \oplus 2T_{1g} \oplus T_{2g}$.[16] The actual states are listed in Table I. The subscript g will be henceforth omitted since we will always refer to even representations.

We begin by considering the nearest neighbour antiferromagnetic (AF) exchange interaction. $\mathcal{J}\sum_{<ab>} \vec{J}_a \cdot \vec{J}_b$ is isotropic, therefore it reduces the degeneracy of the 16-fold collective angular momentum states without mixing the different representations. To calculate the matrix elements, $\vec{J}_a$ must be expressed in terms of the angular momentum quantisation axes (the C_3-axis of each Tb ion). In the following, J_{ai} will always refer to the i-axis ($i = x, y, z$) using the local coordinate axes of the a position ($a = 1, 2, 3, 4$), while J_a^i (used below, in the discussion of neutron scattering) refers to global axes. For the specific choice of axes for the 1 and 2 positions,

$$\begin{aligned} \hat{x}_1 &= (1,1,-2)/\sqrt{6}, \quad \hat{x}_2 = (-1,-1,-2)/\sqrt{6} \\ \hat{y}_1 &= (-1,1,0)/\sqrt{2}, \quad \hat{y}_2 = (1,-1,0)/\sqrt{2} \\ \hat{z}_1 &= (1,1,1)/\sqrt{3}, \quad \hat{z}_2 = (-1,-1,1)/\sqrt{3}, \end{aligned} \qquad (2)$$

one finds

$$\begin{aligned} \vec{J}_1 \cdot \vec{J}_2 \;=\; & -\frac{1}{3}J_{1z}J_{2z} \\ & -\frac{\sqrt{2}}{3}[J_{1z}(J_{2+}+J_{2-}) + (J_{1+}+J_{1-})J_{2z}] \\ & +\frac{1}{3}(J_{1+}J_{2+} + J_{1-}J_{2-}) \\ & -\frac{1}{6}(J_{1+}J_{2-} + J_{1-}J_{2+}). \end{aligned} \qquad (3)$$

$\|A_1\rangle = (\|++--\rangle + \|+-+-\rangle + \|+--+\rangle + \|-++-\rangle + \|-+-+\rangle + \|--++\rangle)/\sqrt{6}$
$\|E^{(1)}_+\rangle = \|++++\rangle$
$\|E^{(1)}_-\rangle = \|----\rangle$
$\|E^{(2)}_+\rangle = (\|+---\rangle + \|-+--\rangle + \|--+-\rangle + \|---+\rangle)/2$
$\|E^{(2)}_-\rangle = \|+++-\rangle + \|++-+\rangle + \|+-++\rangle + \|-+++\rangle)/2$
$\|E^{(3)}_+\rangle = (\|++--\rangle + \varepsilon\|+-+-\rangle + \varepsilon^2\|+--+\rangle + \|-++-\rangle + \varepsilon\|-+-+\rangle + \varepsilon^2\|--++\rangle)\sqrt{6}$
$\|E^{(3)}_-\rangle =$ c.c.
$\|T^{(1)}_{1x}\rangle = (\varepsilon^2[-\|+++-\rangle + \|++-+\rangle + \|+-++\rangle - \|-+++\rangle] + \varepsilon[\|+---\rangle - \|-+--\rangle - \|--+-\rangle + \|---+\rangle])/2\sqrt{2}$
$\|T^{(1)}_{1y}\rangle = (\varepsilon[\|+++-\rangle - \|++-+\rangle + \|+-++\rangle - \|-+++\rangle] + \varepsilon^2[\|+---\rangle - \|-+--\rangle + \|--+-\rangle - \|---+\rangle])/2\sqrt{2}$
$\|T^{(1)}_{1z}\rangle = (\|+++-\rangle + \|++-+\rangle - \|+-++\rangle - \|-+++\rangle + \|+---\rangle + \|-+--\rangle - \|--+-\rangle - \|---+\rangle)/2\sqrt{2}$
$\|T^{(2)}_{1x}\rangle = (\|+--+\rangle - \|-++-\rangle)/\sqrt{2}$
$\|T^{(2)}_{1y}\rangle = (\|+-+-\rangle - \|-+-+\rangle)/\sqrt{2}$
$\|T^{(2)}_{1z}\rangle = (\|++--\rangle - \|--++\rangle)/\sqrt{2}$
$\|T_{2x}\rangle = (\varepsilon^2[-\|+++-\rangle + \|++-+\rangle + \|+-++\rangle - \|-+++\rangle] - \varepsilon[\|+---\rangle - \|-+--\rangle - \|--+-\rangle + \|---+\rangle])/2\sqrt{2}$
$\|T_{2y}\rangle = (\varepsilon[\|+++-\rangle - \|++-+\rangle + \|+-++\rangle - \|-+++\rangle] - \varepsilon^2[\|+---\rangle - \|-+--\rangle + \|--+-\rangle - \|---+\rangle])/2\sqrt{2}$
$\|T_{2z}\rangle = (\|+++-\rangle + \|++-+\rangle - \|+-++\rangle - \|-+++\rangle - \|+---\rangle - \|-+--\rangle + \|--+-\rangle + \|---+\rangle)/2\sqrt{2}$

TABLE I: Basis functions of the collective angular momentum states for the four Tb ion sites, labeled according to the irreducible representations of O_h by which they transform. $\varepsilon = \exp(2\pi i/3)$.

For the axes of the 3 and 4 positions,

$$\begin{aligned} \hat{x}_3 = (-1,1,2)/\sqrt{6}, \quad \hat{x}_4 = (1,-1,2)/\sqrt{6} \\ \hat{y}_3 = (1,1,0)/\sqrt{2}, \quad \hat{y}_4 = (-1,-1,0)/\sqrt{2} \\ \hat{z}_3 = (-1,1,-1)/\sqrt{3}, \quad \hat{z}_4 = (1,-1,-1)/\sqrt{3} \end{aligned} \tag{4}$$

some non-trivial phases appear:

$$\begin{aligned} \vec{J}_1 \cdot \vec{J}_3 \;=\; & -\frac{1}{3} J_{1z} J_{3z} \\ & -\frac{\sqrt{2}}{3}[J_{1z}(\varepsilon J_{3+} + \varepsilon^2 J_{3-}) + (\varepsilon J_{1+} + \varepsilon^2 J_{1-}) J_{3z}] \\ & +\frac{1}{3}(\varepsilon^2 J_{1+} J_{3+} + \varepsilon J_{1-} J_{3-}) \\ & -\frac{1}{6}(J_{1+} J_{3-} + J_{1-} J_{3+}) \end{aligned} \tag{5}$$

$$\begin{aligned} \vec{J}_1 \cdot \vec{J}_4 \;=\; & -\frac{1}{3} J_{1z} J_{4z} \\ & -\frac{\sqrt{2}}{3}[J_{1z}(\varepsilon^2 J_{4+} + \varepsilon J_{4-}) + (\varepsilon^2 J_{1+} + \varepsilon J_{1-}) J_{4z}] \\ & +\frac{1}{3}(\varepsilon J_{1+} J_{4+} + \varepsilon^2 J_{1-} J_{4-}) \\ & -\frac{1}{6}(J_{1+} J_{4-} + J_{1-} J_{4+}) \end{aligned} \tag{6}$$

where $\varepsilon = \exp(2\pi i/3)$. The expression for $\vec{J}_2 \cdot \vec{J}_3$ is similar to $\vec{J}_1 \cdot \vec{J}_4$, etc. The matrix elements are

$$\langle \pm | J_z | \pm \rangle \;\equiv\; \pm j \tag{7}$$

$$\langle \pm | J_\pm | \mp \rangle \;\equiv\; t \tag{8}$$

For the states given in Eq. 1, $j = -3.69\hbar$ and t is exactly zero (this is why the spins are Ising-like). The $E^{(1)}$ states have the lowest energy $-2\mathcal{J}j^2$, while the $E^{(2)}$, $T_1^{(1)}$ and T_2 states have zero energy, and the A_1, $E^{(3)}$ and $T_1^{(2)}$ states have energy $2\mathcal{J}j^2/3$. Note that any linear combination of A_1, $E^{(3)}$ and $T_1^{(2)}$ resembles the "spin ice" state (two spins pointing in and two spins pointing out of each tetrahedron), which is the ground state for ferromagnetic exchange on classical spins. The $E^{(1)}_\pm$ states resemble the classical states often described in the literature as the spins pointing outward from the corners of the cube which contains the tetrahedron, which also minimise the AF exchange energy.

Because $t = 0$, the exchange interaction leads to no mixing between states listed in Table I belonging to the same representation, although this would be permitted under general considerations of symmetry. Non-zero matrix elements that mix $|+\rangle$ and $|-\rangle$ states could originate from mixing with higher crystal field levels[11] or with higher multipole interactions, beginning with quadrupole. Obviously such effects are relevant if the exchange interaction constant $\mathcal{J}$ is small. If $t \neq 0$ then the mixing between states due to the exchange interaction is easily found using the matrix elements given in Table III, below. The dipole-dipole interaction, when limited to a single tetrahedron, only renormalises the exchange interaction, with slight differences between the diagonal and off-diagonal matrix elements of the sixteen collective angular momentum states.

To determine which of the sixteen states is the most likely ground state for $Tb_2Ti_2O_7$ we compare the diffuse neutron scattering intensity pattern with calculations of the scattering function. In the dipole approximation, the scattering intensity is proportional to[17]

$$I(\mathbf{q}) \propto e^{-2W(q)} |F(\mathbf{q})|^2 \sum_m e^{-E_m/k_B T} f_m(q) \tag{9}$$

where $W(q)$ is the Debye-Waller factor, $F(\mathbf{q})$ is the form

factor for Tb^{3+} and

$$f_m(\mathbf{q}) = \sum_{i,j}\sum_{a,b}\sum_{n}(\delta^{ij}-\hat{q}^i\hat{q}^j)\langle m|J_a^i|n\rangle\langle n|J_b^j|m\rangle e^{i\mathbf{q}\cdot(\mathbf{r}_b-\mathbf{r}_a)}. \tag{10}$$

a and b are the four sites at the corners of the tetrahedron and n and m are the sixteen states, whose energy differences are assumed to lie within the energy range across which the neutron scattering is integrated. The functions $f_m(\mathbf{q})$ were calculated for each state m and the results for states belonging to the same doublet or triplet were added. The cases $j \neq 0$ and $t \neq 0$ were considered separately. The calculations yield four different patterns, shown in Fig. 1. The correspondence between different patterns and states is summarised in Table II.

state	j	t
A_1	a)	b)
$E^{(1)}$	−a)	
$E^{(2)}$		b)
$E^{(3)}$	a)	−b)
$T_1^{(1)}$		c)
$T_1^{(2)}$	a)	
T_2		d)

TABLE II: The first column lists the states given in Table I, and the second and third columns indicate to which pattern of Fig. 1 each state corresponds, for non-zero j ($t = 0$) and non-zero t ($j = 0$) respectively. A negative sign indicates that the intensity is reversed, and no entry indicates that the pattern has a uniform intensity.

If the exchange interaction plays a dominant role in this system then one would expect that Fig. 1a), which is associated with the anti-ferromagnetic state $E^{(1)}$ and the ferromagnetic states A_1, $E^{(3)}$ and $T_1^{(2)}$ for $j \neq 0$, would match diffuse neutron scattering measurements. However, this is clearly not the case. Neutron scattering patterns oscillate in three directions, $[0, 0, l]$, $[0, l, l]$ and $[l, l, l]$, and show a broad peak at the position $[0, 0, 2]$.[10] The only figure which shows a qualitative agreement to experiment is Fig. 1c), and in fact the agreement is very good. Considering that the experimental results are a sum over all $f_m(\mathbf{q})$, weighted by the factor $\exp(-E_m/k_BT)$, we conclude that the configuration leading to Fig. 1c) is the ground state.

Fig. 1c) comes from the state $T_1^{(1)}$, which is neither ferro-magnetic nor anti-ferromagnetic and completely insensitive to the parameter j. This result is difficult to explain, but at least it is self-consistent. The interaction which could lead to a $T_1^{(1)}$ type ground state is unknown, but obviously it must contain an effective non-zero t. Likewise, the neutron scattering pattern shown in Fig. 1c) can only be derived with a non-zero t. Moreover, a non-zero t restores the true quantum mechanical nature of this system, for without it only classical Ising-like spins remain.[4,18]

The origin of non-zero t is still an open question but there are a couple of possibilities worth considering. First, higher order multipole interactions restore quantum effects since the matrix elements

$$\langle -|J_zJ_-|+\rangle = \langle -|J_-J_z|+\rangle = -5.21\hbar^2 \tag{11}$$

and

$$\langle -|J_+^2|+\rangle = -0.71\hbar^2 \tag{12}$$

are non-zero. Alternatively, extending the 16-dimensional manifold to include higher crystal electric field levels will add some non-zero matrix elements for the $J_\pm$ operators. This approach was followed in Ref. 11 by including the first excited crystal electric field doublet, thus increasing the number of collective angular momentum states from 16 to 256. In that case, the calculated diffuse neutron scattering intensity pattern agreed well with experiment but a singlet ground state was found based on exchange and dipole-dipole interactions.

The effect of a non-zero t on the exchange interaction on the 16 states given in Table I can be calculated using (3) (5) and (6). The results are summarised in Table III. The lowest energy state is found in the E sector for any values of j and t. Therefore, introducing a non-zero t into the exchange interaction rearranges the energy levels but never produces a T_1 ground state.

Sector	Exchange matrix	$t = 0$	$j = 0$
A_1	$2j^2/3 - 2t^2/3$	$2j^2/3$	$-2t^2/3$
E	$\begin{pmatrix} -2j^2 & 0 & t^2\sqrt{2/3} \\ 0 & -t^2/2 & -4tj/\sqrt{3} \\ t^2\sqrt{2/3} & -4tj/\sqrt{3} & 2j^2/3+t^2/3 \end{pmatrix}$	$2j^2/3$ 0 $-2j^2$	t^2 $-t^2/2$ $-2t^2/3$
T_1	$\begin{pmatrix} -t^2/2 & 0 \\ 0 & 2j^2/3 \end{pmatrix}$	$2j^2/3$ 0	0 $-t^2/2$
T_2	$5t^2/6$	0	$5t^2/6$

TABLE III: Matrix elements for the exchange interaction for each representation within the 16-state manifold spanned by the states in Table I. The last two columns give the eigenvalues of the matrices for $t = 0$ and $j = 0$ respectively.

To summarise, we have classified the low energy collective angular momentum states of the Tb^{3+} ions according to the irreducible representations of the octahedral point group O_h. Diffuse neutron scattering patterns are best described by the $T_1^{(1)}$ ground state. This result cannot be accounted for by the exchange interaction. Then, two important questions remain, namely, what is the nature of the local interactions leading to such a ground state, and what are the low-lying excitations responsible for spin liquid behaviour.

Acknowledgments

I thank Michel Gingras, Martin Plumer and Ivan Sergienko for valuable discussions. This work was sup-

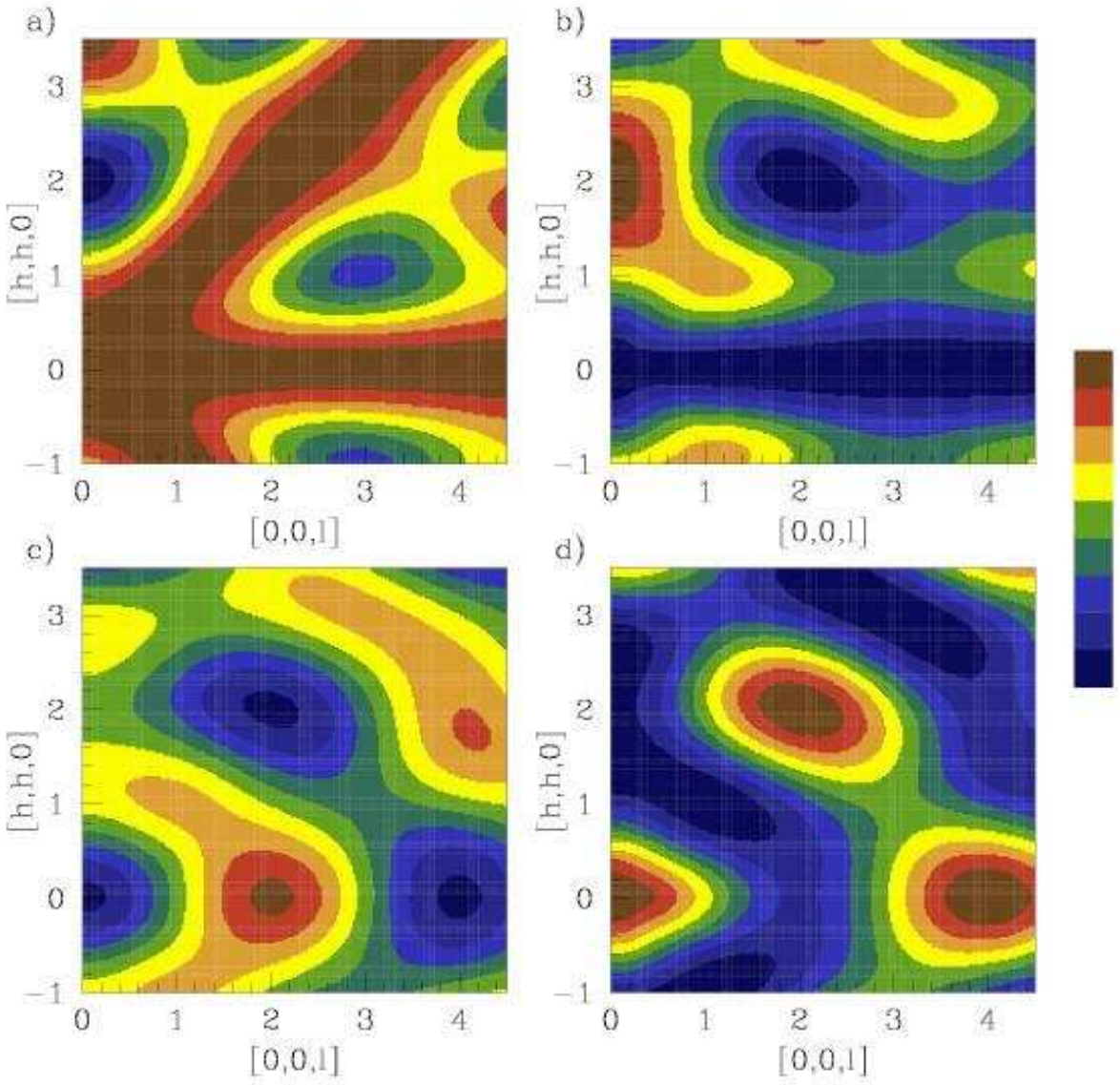

FIG. 1: (Colour) Contour plots of diffuse neutron intensity patterns $f_m(\mathbf{q})$ (Eq. 10) for different states for non-zero j (figure a) and non-zero t (figures b-d) (refer to Table II.) In all four figures the intensities have been scaled in order to draw them using the same colour range.

ported by NSERC of Canada.

* Electronic address: curnoe@physics.mun.ca

[1] J. S. Gardner, A. Keren, G. Ehlers, C. Stock, E. Segal, J. M. Roper, B. Fak, M. B. Stone, P. R. Hammar, D. H. Reich and B. D. Gaulin, *Phys. Rev. B* **68**, 180401(R) (2003).

[2] M. J. P. Gingras, B. C. den Hertog, M. Faucher, J. S. Gardner, S. R. Dunsiger, L. J. Chang, B. D. Gaulin, N. P. Raju and J. E. Greedan, *Phys. Rev. B* **62**, 6496 (2000).

[3] B. C. den Hertog and M. J. P. Gingras, *Phys. Rev. Lett.* **84**, 3430 (2000).

[4] Y.-J. Kao, M. Enjalran, M. Del Maestro, H. R. Molavian and M. J. P. Gingras, *Phys. Rev. B* **68**, 172407 (2006).

[5] Y. Yasui, M. Kanada, M. Ito, H. Harashina, M. Sato, H. Okumura, K. Kakurai and H. Kadowaki, *J. Phys. Soc. Jpn.* **71**, 599 (2002).

[6] N. Hamaguchi, T. Matsushita, N. Wada, Y. Yasui and M. Sato, *Phys. Rev. B* **69**, 132413 (2004).

[7] G. Luo, S. T. Hess and L. R. Corruccini, *Phys. Lett.* **291**, 306 (2001).

[8] Y. M. Jana, O. Sakai, R. Higashinaka, H. Fukazawa, Y. Maeno, P. Dasgupta and D. Ghosh, *Phys. Rev. B* **68**, 174413 (2003).
[9] J. S. Gardner, S. R. Dunsiger, B. D. Gaulin, M. J. P. Gingras, J. E. Greedan, R. F. Kiefl, M. D. Lumsden, W. A. MacFarlane, N. P. Raju, J. E. Sonier, I. Swainson and Z. Tun, *Phys. Rev. Lett.* **82**, 1012 (1999).
[10] J. S. Gardner, B. D. Gaulin, A. J. Berlinsky, P. Waldron, S. R. Dunsiger, N. P. Raju and J. E. Greedan, *Phys. Rev. B* **64**, 224416 (2001).
[11] H. R. Molavian, M. J. P. Gingras and B. Canals, cond-mat/06085321; accepted for publication in *Phys. Rev. Lett.*
[12] P. W. Anderson, *Phys. Rev.* **102**, 1008 (1956).
[13] M. J. Harris, S. T. Bramwell, D. F. McMorrow, T. Zeiske and K. W. Godfrey *Phys. Rev. Lett.* **79**, 2554 (1997).
[14] We use the notation found in M. Tinkham, *Group Theory and Quantum Mechanics* (McGraw-Hill, 1964).
[15] As written, this is imprecise, because the $|\pm 4\rangle$ state has contributions from both the ${}^7F_6$ (Hund's rules) manifold and the ${}^5G_6$ manifold.[2]
[16] Strictly speaking, this decomposition is for the $\mathbf{k} = 0$ representations of the space group. In the following, interactions over a single tetrahedron are discussed. Then, the degeneracy lifting is described in terms of representations of the tetrahedral point group T: $A \oplus 3E \oplus 3T$. There is no additional degeneracy lifting, and the states listed in Table I remain a valid basis for this discussion.
[17] J. Jensen and A. R. Mackintosh, *Rare Earth Magnetism* (Oxford University Press, 1991)
[18] M. Enjalran and M. J. P. Gingras, *Phys. Rev. B* **70**, 174426 (2004).